Est. 1984

ORIENTAL JOURNAL OF CHEMISTRY
An International Open Access, Peer Reviewed Research Journal

www.orientjchem.org

ISSN: 0970-020 X
CODEN: OJCHEG
2022, Vol. 38, No.(5):
Pg. 1183-1191

Docking Studies of N-alkylated Indole chalcone derivatives with *Mycobacterium tuberulosis* Enoyl Acyl Carrier Protein Reductase (Inh A) as Potent Antitubercular agents

SHIVAM JOSHI* and NEHA KAWATHEKAR

Shri G. S. Institute of Technology and Sciences, Indore, India.
*Corresponding author E-mail: shivamjoshi.1990@gmail.com

http://dx.doi.org/10.13005/ojc/380513

(Received: June 29, 2022; Accepted: October 02, 2022)

ABSTRACT

The worrisome rise in multi and extensively drug-resistant *Mycobacterium tuberculosis* strains has prompted researchers to look for new, more effective, and safer treatments. A variety of N-alkylated indole chalcone derivatives were docked against the InhA enzyme to achieve this goal. In the present study, the flexible ligand docking simulations were performed on 88 new compounds against the InhA protein with the PDB ID-4TZK by using Glide module. All the docks are considered as well docked as all of them were bound to Ligand binding domain of InhA. The InhA was identified through an in silico docking investigation as a possible molecular target for the N-alkylated indole chalcone derivatives. This work sought to identify possible inhibitors of the Enoyl-ACP reductase (InhA), which regulates the formation of the cell wall in mycobacterium, using in silico methods. Most of the compounds show good Glide score compare to INH as reference drug. Compound (E)-1-(4-bromo-2-hydroxyphenyl)-3-(1-butyl-1H-indol-3-yl) prop-2-en-1-one (S1R8) showed highest GLIDE score (-10.45), (S1R16-10.41), (S1R22-10.17) and (SIR24-10.10) compared to INH (-7.15). The presence of oxygen group in the ring showed hydrogen bond interactions with NAD and Tyr158 residues. Results obtained are valuable for synthesis and therefore biological screening of promising hits.

Keywords: Tuberculosis, Drug resistance, Docking, Indole derivatives, Enoyl ACP Reductase.

INTRODUCTION

Tuberculosis is an infectious illness initiated by *Mycobacterium tuberculosis*, which mostly affects the lungs and has a high fatality rate worldwide.[1] Currently, there is a need for antitubercular agents effective against the drug-resistant strains of *M. tuberculosis*.[2] Today, tuberculosis is one of the top five causes of worldwide death, killing 2 million people each year, according to WHO information sheets.[3] According to worrisome WHO estimates, one billion new active cases will be diagnosed by 2024; if new anti-TB medications are not discovered, TB would spread to every corner of the world.[4] In 2017, about ten million people worldwide contracted tuberculosis, with India, China, and Indonesia accounting for the majority of cases.[5] Globally, an estimated 10 million new tuberculosis cases were recorded in 2019, with reports of drug-resistant TB on the rise.[6] Tuberculosis is a

severe public health issue that competes with the human immunodeficiency virus (HIV) as the leading cause of infectious disease-related death globally. Although there has been a downward trend in TB incidence, prevalence, and death over the previous decade, global TB eradication remains a long way off, and enormous resource commitment is still necessary.[7] Two major reasons are sustaining and fueling the present tuberculosis epidemic: HIV disease and its link to active TB illness, and increase in ignorance of *Mycobacterium tuberculosis* strains to the most active anti-TB medicines.[8] Finding new tuberculosis drug candidates and druggable targets has become more important since multidrug-resistant and exceptionally drug-resistant (XDR) strains of *M. tuberculosis* have become more prevalent.[9] Resistance has surfaced for all clinically prescribed antitubercular drugs.[10]

Current anti-TB medication, including first-line is about 50 years old, yet it still needs 6 months of treatment and 20 months in the event of Multidrug resistant-TB (MDR-TB). As a result, new medicines are required to shorten and simplify the treatment process, as well as to increase the efficacy and tolerability of MDR-TB therapy.[11]

The majority of persons with tuberculosis are healed by sticking to a six-month, four-drug anti-TB regimen. However, the bacteria that cause tuberculosis, *Mycobacterium tuberculosis*, can sometimes become resistant to therapy, resulting in anti-TB drug overuse and lowered patient immunity due to poor management.[12] Multidrug resistance happens when both Isoniazid and Rifampicin fail to work against Tuberculosis infection. XDR TB is a very uncommon kind of drug-resistant tuberculosis. Isoniazid and Rifampin, as well as any fluoroquinolone derivatives and at least one of three parenteral second line medicines, are all resistant to XDR TB (i.e., AMK, KANA, CAPRE).[13]

Docking

Docking is a method for determining the small molecule's affinities and functionality as well as the direction in which it will attach to its protein targets. As a result, docking is critical in rational drug design.[14] Rigid Docking The search space is highly constrained when the moiety and active site are together regarded as unbending entities, with only three conveyance and three rotating points of liberty.[15] Flexible Docking It's critical to deliberate the flexibility of both the Molecule and the protein in systems that follow the induced fit paradigm, because both the Ligand and the receptor change conformations to form a minimum energy perfect-fit combination.[15]

Computational studies of compounds with crystal structure of *M.Tb* enoyl acp reductase (INHA)

Docking studies

Docking studies performed in the Computer added drug design lab, Department of Pharmacy, SGSITS, Indore with the help of GLIDE version 9.2 module of Schrödinger software running on multiprocessor-window PC. The crystal structure of *Mycobacterium TB* enoyl reductase complexed with cyclohexyl oxopyrrolidine carboxamide derivatives, which was taken from Protein Data Bank, was subjected to docking recreations.

Ligand preparation

The chosen ligands were illustrated using the 2D Sketcher in Schrödinger Maestro ("Maestro, version 9.1, 2010), and the energy-minimized 3D molecular structures were produced using the LigPrep tool. Using Epik in LigPrep, the Tautomers and ionization state of the Molecule were measured at neutral pH. Each Ligand produced a maximum of 32 stereoisomers, each with a unique low-energy ring conformation.

For all ligands, three-dimensional (3D) coordinates have been created with LigPrep. With either a couple of fast rule centered programs (ionization and tautomerism) or with E-pik, ionization/ tautomeric states were formed, which is focused towards the more precise method Hammett and Taft. Besides the estimate of rationale, Epik is also calculating a penalty to measure the Ligand states, Energetic costs are needed to solve each state. In units of kcal/mol, the Epik state penalty is determined, it is thus directly consistent with Glide Score Used for docking and enabling us to explore the effect of the Epik State Penalty is applied to the Glide Score. The sum of the punishment for Glide Score and the state of Epik has alluded to as the Docking Score in Glide. For determining final ranking and enrichment calculations Docking Score is used. Epik also has a system for handling metallic binding states, which requires increasing the pH spectrum for the stage of state production and then reducing the

penalties for states in the docking process where the bonding to a metal ion satisfies a negative charge.

Protein structure preparation

For the purpose of performing docking calculations, the crystalline arrangement of *Mycobacterium Tb* enoyl reductase attached with 1-cyclohexyl-N-(3,5-dichlorophenyl)-5-oxopyrrolidine-3-carboxamide (PDB ID 4TZK) was employed. The co-factor NAD was retained during docking, while H_2O molecules were removed. Protein is imported to the workspace after selecting the 'import option' from the Project menu. The 'show table' option is selected from the menu, and then the table protein is selected from the table to receive the specified protein on the workspace. Protein Preparation Wizard is selected in Maestro 9.1. Preprocess is then selected in a new window. All water molecules that are unattached to the protein are eliminated during review and modification. The Ligand-containing protein chain is picked, and the rest is removed. After that, click 'Generate States.' then, refines is selected, and 'exhaustive sampling' is checked, before clicking optimize to begin. Then the 'minimize' button is pressed, followed by the start button. The Flip/NoFlip model is obtained after the entire process is completed.

Grid generation

Using Maestro 9.1, Ligand and Flip/NoFlip model is prepared. Once they are prepared, from the application menu, 'glide option' is selected and in sub-menu 'Receptor Grid Generation' is selected. A new window appears, 'Pick to identify ligand' is then selected and in the workspace, the ligand is picked by double-clicking on the ligand. Once the ligand is selected, 'Site Option' is selected and the size of the grid is adjusted in such a way that ligands fit in the grid. Once done 'Constraints menu' and 'Rotatable Group' are selected and then the start is clicked. In the new window, the desired name is entered and the start is then clicked. On completion of the process glide grid model is generated. Gide generation is showing in Figure 1.

Glide docking

The GLIDE program's "Extra Precision" (XP) mode was used to complete all docking calculations. The joining spot, for which the varied energy grids were determined and kept, is characterized by two centered cubes: the scale factor for van der Waals radii was applied to atoms with absolute partial charges less than or equal to 0, with a Root Mean Square Deviation of less than 0.5 and a highest atomic displacement of less than ligand and protein. The frame, which must contain the center of any acceptable ligand position, and the bounding box, which must include all ligand atoms of an acceptable pose, were removed as terminated in order to increase variety in the retained grids. At most 32 poses per ligand were created when each docking calculation was completed. A GLIDE score (Gscore) function was used to select the best docked structure. Another scoring function used by GLIDE is the Emodel, which is produced by combining the GLIDE score, dipole induced Dipole interactions, Coulombic, and the ligand's resilience. Fig. 2 depicts the interactions of a designed ligand with a protein.

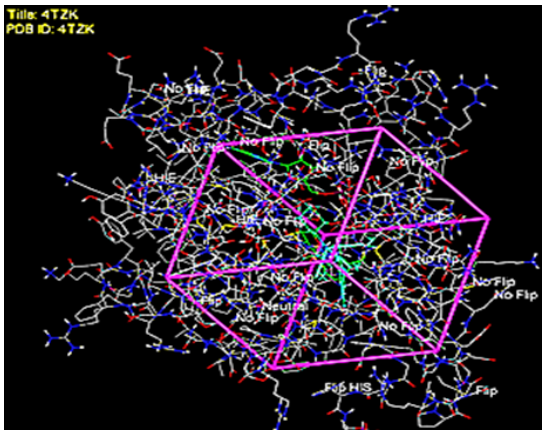

Fig. 1. Glide Gride Generation

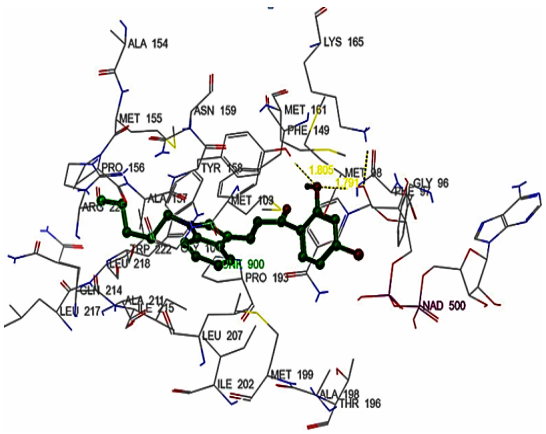

Fig. 2. Ligand (S1R8) interaction with protein (4TZK)

QikProp analysis

Every hour, QikProp analyses more than half a million compounds for pharmaceutically

significant features, creating it a crucial tool for lead generation and improvement. Precise prediction of ADME properties can completely eliminate pointless experiments on compounds that will end in failure prior to costly investigational events like HTS. The desirable features of a particular compound can be strengthened by focusing lead optimization efforts with the help of ADME estimate. The chemical should have significant scientific effects at low effective doses, minimal harmful effects, and the capacity to continue acting until the desired effect is seen in order to be a successful medication. For a better pharmacokinetic profile, the ADME features of drug candidates are taken into account during the drug discovery process.

SiteMap analysis

Researchers may effectively locate binding sites and anticipate their pharmacological ability with the use of the SiteMap established method for binding site identification and evaluation. By providing knowledge about ligand-receptor collaborations, SiteMap also helps with lead optimization by recommending effective methods for lead molecule modification that will increase receptor complementarity. The sitemap analysis is directly connected to Pfizer's rule RO5, in the sitemap results hydrophobic region indicate by yellow colour net, H-bond contributor blue network, and H-bond adherent red colour mesh. Fig. 3 and 4 are showing site map analysis of designed compounds.

RESULT AND DISCUSSION

To understand the relative chemicals' order of activity, S1R1-SIR24, S2R1-S2R32, and S3R1-S3R32 were docked into the mycobacterial enoyl reductase binding site. The two primary factors to be considered while performing docking are the highest score, or posture with the highest rank, and the best pose, or posture with the lowest RMSD to the reference ligand from the experimentally determined structure. Some compounds' docking scores between -10.29 and -7.0 were deemed satisfactory. The findings in Table 2 made it abundantly evident that substances had strong affinity for the Mycobacterium tuberculosis Enoyl ACP protein (4TKZ). The most active compound's docking scores were discovered to be -10.45 (SIR8), -10.41 (S1R16), -10.10 (S1R24), and -10.17. (S1R22).

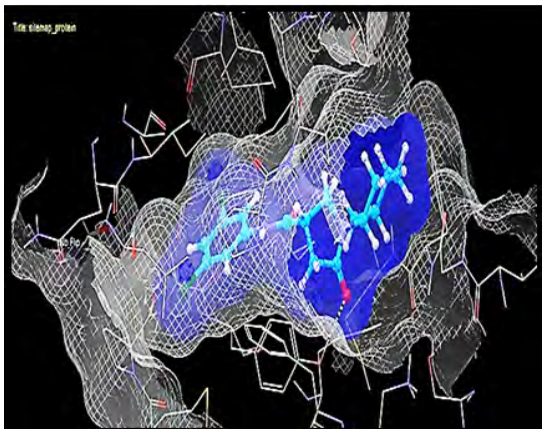

Fig. 4. Sitemap protein interaction with incorporated ligand

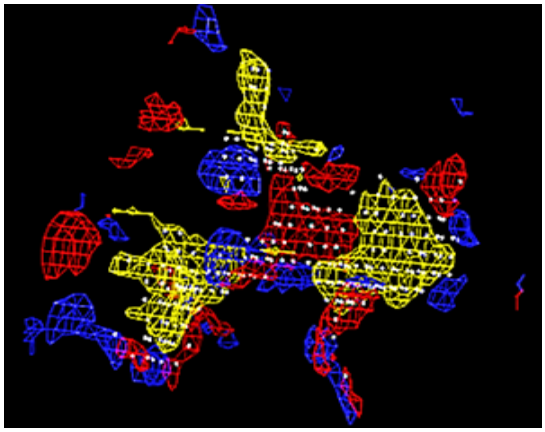

Fig. 5. Sitemap analysis

Table 1: ADME properties

Code	Absorption			Distribution		Metabolism	ExcretionTotal clearance (log ml/min/kg)
	LogS(logmol/L)	Caco-2 perm.	Int.abs(%abs)	VDss(logL/kg)	BBB perm		
S1R8	-6.021	0.945	91.668	0.481	-0.086	A*, B#, C□, Dπ	0.101
S1R16	-6.274	0.945	91.167	0.552	-0.136	A*, B#, C□, Dπ	0.131
S1R22	-4.804	0.736	92.292	-0.033	-0.116	A*, B#, C□, Dπ	0.564
S1R24	-6.161	0.956	91.756	0.468	-0.047	A*, B#, C□, Dπ	-0.004
S3R3	-6.567	0.965	92.079	-0.337	0.074	B#, C□, Dπ, E@	0.458
S1R14	-4.965	0.675	91.674	0.03	-0.206	A*, B#, C□, Dπ`	0.616

S1R9	-6.686	1.051	94.323	0.71	0.626	A*, B#, C□, Dπ	0.551
S1R3	-5.437	1.314	92.771	0.456	-0.037	A*, B#, C□, Dπ	0.615
S1R10	-6.763	0.994	93.217	0.972	0.559	A*, B#, C□, Dπ	-0.003
S1R18	-6.71	1.004	93.836	0.874	0.475	A*, B#, C□, Dπ	-0.138
S1R13	-6.778	1.007	93.23	0.994	0.526	A*, B#, C□, Dπ	0.115
S1R15	-6.754	1.018	93.664	0.975	0.497	A*, B#, C□, Dπ	0.117
S1R7	-6.512	1.018	94.165	0.887	0.456	A*, B#, C□, Dπ	0.088
S1R6	-4.734	0.716	92.174	-0.017	-0.156	A*, B#, C□, Dπ	0.594
S1R1	-6.365	1.375	94.835	0.629	0.585	A*, B#, C□, Dπ,Fβ	0.53
S1R21	-6.71	1.004	93.836	0.874	0.475	A*, B#, C□, Dπ	-0.138
S1R11	-5.756	1.004	92.27	0.527	-0.087	A*, B#, C□, Dπ	0.636
S1R5	-6.538	1.007	93.731	0.908	0.485	A*, B#, C□, Dπ	0.085
S1R4	-6.915	0.991	92.818	0.906	0.516	A*, B#, C□, Dπ	0.103
S1R12	-7.129	0.991	92.317	0.991	0.557	A*, B#, C□, Dπ	0.133
S1R23	-6.703	1.029	94.282	0.877	0.414	A*, B#, C□, Dπ	-0.017
S3R14	-5.597	0.652	90.865	-0.847	-0.319	A*, B#, C□, Dπ	0.43
S3R22	-6.658	0.88	90.543	-0.267	0.063	A*, B#, C□, Dπ	0.103
S1R2	-6.521	0.994	93.718	0.884	0.518	A*, B#, C□, Dπ	-0.033
S3R27	-6.292	0.491	93.241	-0.397	-0.423	A*, B#, C□, Dπ	0.48
S3R7	-7.179	0.963	92.911	0.15	0.184	A*, B#, C□, Dπ	0.138
S3R6	-5.578	0.583	90.655	-0.912	-0.304	A*, B#, C□, Dπ	0.427
S3R32	-6.431	0.449	91.495	-0.394	-0.394	A*, B#, C□, Dπ	0.079
S3R16	-6.658	0.88	90.543	-0.267	0.063	A*, B#, C□, Dπ	0.103
S1R19	-5.575	1.015	92.889	0.443	0.003	A*, B#, C□, Dπ	0.584
S2R1	-7.283	1.021	96.148	0.083	0.695	A*, B#, C□	0.456
S3R30	-5.199	0.671	91.816	-0.944	-0.574	A*, B#, C□, Dπ	0.449
S2R11	-6.28	0.976	93.811	-0.203	0.068	A*, B#, C□, Dπ, E@	0.536
S3R5	-7.12	0.977	93.839	0.182	0.155	A*, B#, C□, Dπ	0.139
S1R17	-6.554	1.384	94.941	0.62	0.543	A*, B#, C□, Dπ	0.5
S3R29	-7.124	0.974	95	0.105	-0.033	A*, B#, C□, Dπ	0.057
S3R8	-6.652	0.889	90.334	-0.335	0.095	A*, B#, C□, Dπ	0.16
S3R25	-6.923	1.008	95.293	-0.174	0.105	A*, B#, C□, Dπ	0.411
S3R9	-7.207	1.003	94.342	-0.017	0.261	A*, B#, C□, Dπ	0.391
S2R14	-5.316	0.648	93.214	-0.834	-0.051	A*, B#, C□, Dπ, E@	0.515
S3R1	-7.165	1.012	94.132	-0.083	0.293	A*, B#, C□, Dπ	0.389
S3R26	-7.155	0.97	94.373	0.08	-0.049	A*, B#, C□, Dπ	-0.061
S3R13	-7.136	0.969	94.049	0.247	0.124	A*, B#, C□, Dπ	0.082
S3R21	-6.585	0.219	92.021	-0.021	-0.74	A*, B#, C□, Dπ	0.043
S3R10	-7.167	0.965	93.421	0.222	0.108	A*, B#, C□, Dπ	-0.036
S2R3	-6.228	0.975	94.095	-0.185	0.084	A*, B#, C□, Dπ,E@	0.54
S1R20	-7.1	1.001	92.935	0.896	0.473	A*, B#, C□, Dπ	-0.002
S3R31	-7.169	0.959	94.073	0.071	-0.004	A*, B#, C□, Dπ	0.056
S3R15	-7.191	0.954	93.121	0.213	0.152	A*, B#, C□, Dπ	0.08
S3R18	-6.608	0.27	91.393	-0.039	-0.759	A*, B#, C□, Dπ	-0.075
S2R9	-7.342	1.022	95.863	0.067	0.691	A*, B#, C□,	0.452
INH	-2.024	0.695	96.452	0.053	-0.002	-	0.703

Note- A*-CYP3A4 substrate, B#-CYP1A2, C□- CYP2C19, Dπ- CYP2C9 inhibitors, E@- CYP2D6 inhibitors, Fβ-CYP3A4 inhibitors

Table 2: Pharmacokinetic analysis

Code	Lipinski's Rule of 5					Veber Rule	
	Log P	H donor	H acceptor	Mol. Wt	No. of Violation	TPSA(A^2)	No. of rotatable bonds
S1R8	3.91	1	2	398.29	0	42.23	6
S1R16	4.33	1	2	412.32	0	42.23	7
S1R22	3.33	2	3	347.41	0	62.46	5
S1R24	3.82	1	2	410.30	0	42.23	5
S3R3	2.83	1	3	381.42	0	59.30	6
S1R14	3.54	2	3	349.42	0	62.46	7
S1R9	3.76	0	2	335.41	1	22.00	7

S1R3	3.22	1	2	319.40	0	42.23	6
S1R10	3.98	0	1	396.32	1	22.00	7
S1R18	3.95	0	1	394.30	1	22.00	5
S1R13	3.98	0	1	396.32	1	22.00	7
S1R15	3.97	0	1	396.32	1	22.00	7
S1R7	3.83	0	1	382.29	1	22.00	6
S1R6	3.01	2	3	335.40	0	62.46	6
S1R1	3.57	0	2	321.39	0	22.00	6
S1R21	3.95	0	1	394.30	1	22.00	5
S1R11	3.37	1	2	333.42	0	42.23	7
S1R5	3.91	0	1	382.29	1	22.00	6
S1R4	3.96	0	1	372.29	1	22.00	6
S1R12	4.15	0	1	386.31	1	22.00	7
S1R23	3.97	0	1	394.30	1	22.00	5
S3R14	3.13	2	4	411.45	0	79.53	6
S3R22	1.96	2	6	442.42	0	125.35	7
S1R2	3.91	0	1	382.29	1	22.00	6
S3R27	3.13	1	4	411.45	0	68.53	7
S3R7	3.43	0	2	444.32	0	39.07	6
S3R6	2.58	2	4	397.42	0	79.53	6
S3R32	3.77	1	4	490.37	0	68.53	7
S3R16	3.82	1	3	474.35	0	59.30	6
S1R19	3.22	1	2	331.41	0	42.23	5
S2R1	3.76	0	2	369.43	1	22.00	5
S3R30	3.17	2	5	427.45	0	88.76	7
S2R11	3.36	1	2	367.44	0	42.23	5
S3R5	3.54	0	2	444.32	0	39.07	6
S1R17	3.70	0	2	333.40	1	22.00	5
S3R29	3.71	0	3	474.35	0	48.20	7
S3R8	3.26	1	3	460.32	0	59.30	6
S3R25	3.53	0	4	413.44	0	48.30	7
S3R9	3.56	0	3	397.44	0	39.07	6
S2R14	3.81	2	3	383.44	0	62.46	5
S3R1	3.26	0	3	383.41	0	39.07	6
S3R26	3.71	0	3	474.35	0	48.20	7
S3R13	3.74	0	2	458.35	0	39.07	6
S3R21	2.96	0	4	489.32	0	84.89	7
S3R10	3.74	0	2	458.35	0	39.07	6
S2R3	3.29	1	2	367.44	0	42.23	5
S1R20	4.02	0	1	384.30	1	22.00	5
S3R31	3.71	0	3	474.35	0	48.20	7
S3R15	3.74	0	2	458.35	0	39.07	6
S3R18	2.96	0	4	489.32	0	84.89	7
S2R9	3.74	0	2	369.43	1	22.00	5
INH	-0.96	3	4	137.14	0	69.01	5

Table 3: Docking Results

Sr. No	Ligandcode	GlideScore	GlideEng.	LipophilicEvdW	PhobEn	HBond	Electro	Sitemap	RotPenal
1	S1R8	-10.45	-50.29	-1.92	0.26	-5.59	-0.61	0	-0.43
2	S1R16	-10.41	-48.94	-1.92	0.30	-5.72	-0.56	0	-0.38
3	S1R22	-10.17	-45.71	-1.18	0.34	-5.87	-0.55	0	-0.58
4	S1R24	-10.10	-49.03	-1.30	0.25	-5.60	-0.74	0	-0.58
5	S3R3	-9.82	-37.38	-1.33	0.34	-5.25	-0.46	0	-0.50
6	S1R14	-9.70	-46.80	-1.92	0.40	-5.23	-0.53	0	-0.43
7	S1R9	-9.59	-47.47	-0.7	0.36	-5.91	-0.43	0	-0.53
8	S1R3	-9.54	-45.77	-0.7	0.39	-6.02	-0.27	0	-0.50
9	S1R10	-9.48	-46.81	-0.7	0.27	-5.97	-0.36	0	-0.53
10	S1R18	-9.35	-49.58	-0.41	0.22	-6.04	-0.29	0	-0.63
11	S1R13	-9.32	-44.67	0	0.27	-6.74	-0.17	0	-0.50

12	S1R15	-9.32	-37.84	0	0.27	-6.41	-0.12	-0.30	-0.57
13	S1R7	-9.24	-39.99	0	0.23	-6.22	-0.09	-0.34	-0.59
14	S1R6	-9.24	-33.47	-1.54	0.36	-4.70	-0.53	-0.03	-0.42
15	S1R1	-9.14	-44.73	0	0.31	-6.39	-0.13	0	-0.50
16	S1R21	-9.07	-45.69	-0.43	0.22	-5.85	-0.36	0	-0.46
17	S1R11	-8.97	-21.31	-0.7	0.44	-5.21	-0.27	-0.31	-0.53
18	S1R5	-8.81	-44.53	0	0.23	-5.79	-0.38	0	-0.63
19	S1R4	-8.77	-43.94	0	0.24	-6.26	-0.03	0	-0.46
20	S1R12	-8.61	-32.27	0	0.28	-6.18	0.00	0	-0.50
21	S1R23	-8.54	-42.63	0	0.22	-6.10	-0.12	-0.03	-0.32
22	S3R14	-8.38	-33.88	-0.89	0.30	-4.47	-0.53	-0.21	-0.53
23	S3R22	-8.27	-38.30	-1.18	0.26	-4.51	-0.43	-0.19	-0.29
24	S1R2	-8.23	-47.01	-0.37	0.23	-5.96	-0.31	0	-0.59
25	S3R27	-8.21	-35.55	-0.7	0.30	-4.89	-0.36	-0.20	-0.33
26	S3R7	-8.16	-10.69	-1.18	0.22	-4.30	-0.23	-0.40	-0.24
27	S3R6	-8.13	-28.94	-1.03	0.32	-4.19	-0.53	-0.22	-0.38
28	S3R32	-8.12	-36.63	-0.7	0.22	-4.73	-0.34	-0.21	-0.35
29	S3R16	-7.99	-32.00	-0.7	0.23	-4.42	-0.37	-0.18	-0.55
30	S1R19	-7.91	-36.84	-0.45	0.37	-4.96	-0.06	-0.40	0.00
31	S2R1	-7.81	-31.64	0	0.24	-5.39	0.02	-0.41	0.00
32	S3R30	-7.75	-31.83	-1.25	0.28	-4.65	-0.53	-0.15	-0.37
33	S2R11	-7.74	-17.15	-0.27	0.31	-4.82	-0.11	-0.40	-0.18
34	S3R5	-7.70	-33.64	0	0.22	-4.92	-0.27	-0.16	-0.55
35	S1R17	-7.70	-28.82	0	0.29	-4.27	0.06	-0.71	-0.69
36	S3R29	-7.67	-37.26	0	0.19	-5.26	-0.22	-0.20	-0.34
37	S3R8	-7.66	-32.66	-0.7	0.24	-4.41	-0.35	-0.20	-0.55
38	S3R25	-7.65	-20.64	-0.39	0.25	-4.21	-0.22	-0.45	-0.50
39	S3R9	-7.57	-17.80	-0.30	0.27	-4.25	-0.19	-0.45	-0.48
40	S2R14	-7.56	-21.29	-1.33	0.28	-5.32	-0.32	-0.01	-0.65
41	S3R1	-7.49	-17.95	-0.61	0.28	-4.00	-0.23	-0.40	-0.30
42	S3R26	-7.45	-34.65	0	0.19	-4.83	-0.29	-0.20	-0.32
43	S3R13	-7.42	-33.48	0	0.21	-4.75	-0.28	-0.19	-0.41
44	S3R24	-7.37	-36.58	-0.7	0.21	-4.34	-0.32	-0.20	-0.32
45	S3R21	-7.34	-37.10	0	0.18	-4.76	-0.22	-0.18	-0.36
46	S3R10	-7.28	-31.66	0	0.21	-4.57	-0.31	-0.19	-0.50
47	S2R3	-7.27	-36.23	0	0.31	-4.64	-0.12	-0.40	-0.68
48	S1R20	-7.25	-28.40	0	0.23	-5.83	0.00	0.00	-0.43
49	S3R31	-7.25	-31.38	0	0.19	-4.68	-0.27	-0.17	-0.32
50	S3R15	-7.22	-32.27	0	0.21	-4.46	-0.26	-0.19	-0.53
51	S3R18	-7.15	-34.58	0	0.18	-4.51	-0.24	-0.17	-0.40
52	S2R9	-7.15	-16.13	0	0.24	-4.50	0.00	-0.62	0.00
53	S2R28	-6.91	-26.04	0	0.18	-4.76	0.01	-0.16	-0.35
54	S3R11	-6.87	-16.93	-0.57	0.32	-4.19	-0.28	-0.40	-0.58
55	S2R10	-6.78	-31.08	0	0.18	-4.99	-0.13	-0.16	-0.61
56	S3R23	-6.76	-35.49	0	0.18	-4.52	-0.20	-0.18	-0.38
57	S3R2	-6.64	-32.00	0	0.22	-4.47	-0.25	-0.20	-0.45
58	S2R25	-6.62	-26.81	0	0.22	-4.37	-0.09	-0.17	-0.32
59	S3R12	-6.61	-36.38	0	0.21	-4.85	-0.28	-0.18	-0.50
60	S3R28	-6.59	-35.17	0	0.20	-4.98	-0.29	-0.15	-0.36
61	S2R12	-6.53	-27.13	0	0.19	-4.33	-0.05	-0.18	-0.52
62	S2R17	-6.35	-24.13	0	0.24	-3.99	-0.05	-0.19	-0.45
63	S2R13	-6.24	-28.59	0	0.18	-4.72	-0.09	-0.17	-0.45
64	S3R4	-6.21	-29.55	0	0.23	-4.48	-0.26	-0.14	-0.50
65	S3R17	-5.95	-33.71	0	0.23	-4.52	-0.26	-0.15	-0.40
66	S3R20	-5.92	-36.20	0	0.19	-4.44	-0.22	-0.18	-0.35
67	S2R18	-5.74	-23.97	0	0.18	-3.94	-0.04	-0.18	-0.43
68	S2R26	-5.32	-26.49	0	0.17	-4.38	-0.09	-0.17	-0.34
69	S2R15	-5.14	-24.83	0	0.18	-4.51	-0.03	-0.16	-0.51
70	S2R27	-5.06	-21.40	-0.61	0.28	-3.25	-0.09	-0.11	0.00
71	S2R20	-5.03	-28.20	-0.58	0.19	-3.40	-0.15	-0.22	0.00
72	S2R6	-5.00	-20.41	-1.17	0.28	-3.34	-0.20	-0.19	-0.25

73	S2R23	-4.90	-23.48	0	0.18	-4.15	-0.02	-0.18	-0.48
74	S2R31	-4.65	-27.84	0	0.17	-4.28	-0.04	-0.17	-0.28
75	S2R5	-4.64	-21.23	0	0.18	-3.91	0.03	-0.19	-0.25
76	S2R2	-4.44	-20.09	0	0.18	-3.42	0.08	-0.19	-0.30
77	S2R30	-4.18	-3.98	-1.26	0.26	-2.62	-0.26	-0.19	0.00
78	S2R4	-3.97	-22.34	0	0.19	-3.62	0.03	-0.20	-0.28
79	S2R22	-3.86	-5.16	-1.14	0.28	-2.65	-0.23	-0.21	0.00
80	S3R19	-3.83	-40.20	-0.7	0.28	-4.70	-0.36	-0.21	-0.29
81	S2R19	-3.83	-24.29	-0.59	0.31	-2.69	-0.11	-0.37	0.00
82	S2R21	-3.75	-33.44	0	0.18	-5.12	-0.09	-0.18	-0.48
83	S2R29	-3.17	-33.97	0	0.17	-4.95	-0.06	-0.19	-0.21
84	S2R8	-2.93	-29.15	-0.7	0.22	-4.07	-0.05	-0.21	-0.40
85	S2R7	-2.93	-20.48	0	0.18	-3.60	0.06	-0.19	-0.31
86	INH	-7.15	-40.35	-2.27	-0.5	-0.7	-0.2	-0.4	0

According to the findings, (Table 1) the N-alkylated indole chalcones derivatives have a molar mass of less than 500, ranging from 321.39 to 489.32, indicating that they are more easily metabolized than bigger molecules. The Log P indicates lipophilicity, with values ranging from 1.96-4.33 for N-alkylated indole chalcones derivatives. Indole derivatives' log P values are within the recommended range. All of the compounds had 1-2 H-bond donors and 2-6 H-bond acceptors, which is unusual. When compared to the reference medication, 52 of the 88 compounds created have the best docking result. Out of the 52 best compounds, 37 have been determined to follow the Lipinski Rule and have drug-like pharmacokinetics.

For optimal biological effect, the pharmacokinetic parameters of a medicine should be determined before it is synthesized. As a result, the N-alkylated indole chalcones derivatives were created utilizing the Lipinski and Veber drug-likeness principles. To produce lipophilicity in N-alkylated indole substituted derivatives, the indole scaffold was preserved in all compounds and substituted, fused, and halogen contain aromatic rings were added. Permeation of any medication into the cell wall of Tuberculosis can be done by generating lipophilicity, according to popular belief. Table 1 lists the ADME parameters of N-alkylated indole substituted compounds. Solubility and intestinal permeability were used to assess drug absorption. The logarithm of molar concentration is used to calculate the aqueous solubility of the compounds, and the solubility of proposed compounds ranges from -4.734 to -7.342. The compounds are relatively water soluble because they contain lipophilic functionalities meant to increase cell permeability. Since the majority of an oral medication's absorption occurs in the small intestine, the compounds' percent absorption was estimated. Because human colorectal adenocarcinoma cells resemble intestinal epithelium, Caco-2 permeability can predict oral medicine consumption in general. The intestinal absorption of all the molecules is high, ranging from 90.34 to 95.86%, which is comparable to that of isoniazid.

A volume of distribution (VDss) and penetrability of blood brain hurdle were used to estimate the drug's distribution profile. Higher VDss implies better drug distribution in the tissues than in plasma, and Log VDss>0.45 suggests more tissue distribution. All of the compounds have a moderate tissue distribution; with compound S1R13 having a distribution value that is higher than isoniazid at 0.994.

A drug's percent bound effectiveness indicates how much less it is bound to plasma proteins and how much further freely it can be distributed. To determine the permeability of the BBB, QikProp was employed. As in the case of TB meningitis, BBB penetration is critical because it affects the central nervous system. Isoniazid, on the other hand, does not display any of these interactions with cytochromes, either as a substrate or as an inhibitor. A reduced overall clearance of all of the N-alkylated indole chalcone derivatives was determined and was found to be -0.003 to 0.636 logml/min/kg. The overall clearance of S1R11 is 0.636 logml/min/kg, which is comparable to Isoniazid. All of the compounds display excellent ADME characteristics when compared to INH and can be viewed as prospective lead candidates.

CONCLUSION

The Docking studies of N-alkylated indole chalcones derivatives with InhA protein (4TZK) shows prominent results. The highest Glide scorer compounds (S1R8, S1R16, S1R24 and S1R22) shows Hydrogen bond interaction with TYR 158 amino acid and nicotinamide adenine dinucleotide (NAD), which is essential for activity against the InhA target. The substitution of an electron removing or providing group plays a significant role in this research. The inclusion of electron-withdrawing with donating group groups in substituted phenyl rings of indole chalcone improved the best effects against InhA protein, according to resonance. By using the inductive effect, all halogens can attract electrons from other atoms, resulting in the formation of a dipole moment inside the complex. This can improve a drug's water solubility and allow it to interact with its biological target. The major objective of this work was to demonstrate a clear correlation between structural characteristics and inhibitory action. It was noted and stated that the results were consistent with prior studies. From the molecular docking study, it can be observed that the molecules acquire almost the same sites as reported in an earlier interaction with residues TYR 158. Also glide score, H-bond, Phoben, LipophilicEvdW, and Site map values for all compounds are comparable with that of Reference. As a result, this study serves as a foundation for the development of novel analogues that are more potent InhA antagonists.

ACKNOWLEDGEMENT

The authors extend their appreciation to SGSITS, Department of pharmacy Indore for providing the research amenities.

REFERENCES

1. Alsayed S.S.R; Lun S.; Luna G.; Beh C.C.; Payne A.D.; Foster N., *RSC Advances .,* **2020**,*10*(13), 7523-40.
2. Kar S.S.;Bhat G. V.; Rao P.P. Shenoy V.P.; Bairy I.; Shenoy G.G., *Drug design, development and therapy.,* **2016**, *10*(1), 2299-2310.
3. Patel H.M.; Noolvi M.N.; Sethi N.S.; Gadad A.K.; Cameotra S.S., *Arabian Journal of Chemistry*., **2017**, *10*(1), 996-1002.
4. Rathod A.S.; Reddy P.V.; Biradar J.S., *Russian Journal of Organic Chemistry .,* **2020**, *56*(4), 662-670.
5. Mustaqeem A.M.; Siddiqui N.A.; Mothana R.A.; Nasr F.A.; Almarfadi O.M., *Arabian Journal of Chemistry.,* **2021**,*14*(4), 1030-1034.
6. Dueke-Eze C.U.; Fasina T.M.; Oluwalana A.E.; Familoni O.B.; Mphalele J.M.; Onubuogu C., *Scientific African.,* **2020**, *9*, 522-525.
7. Sulis G.; Roggi A.; Matteelli A.; Raviglione MC., *Tuberculosis*., **2014**, *6*(1), 201-210.
8. Ahmad S., *Clin Dev Immunol*., **2011**, 814-943.
9. Li Z.; Bai X,; Deng Q.; Zhang G.; Zhou L.; Liu Y., *Bioorganic & Medicinal Chemistry .,* **2017**, *25*(1), 213-220.
10. Das S.K.; Panda G.; Chaturvedi V.;, Manju Y.S.; Gaikwad A.K.; Sinha S., *Bioorg Med Chem Lett*., **2007,** *17*(20), 5586-5599.
11. Patel K.N.; Telvekar V.N., *Europeon Journal of Meicinal Chemistry.,* **2014**, *75*(3), 43-56.
12. Seung K.J.; Keshavjee S.; Rich M.L.; *Cold Spring Harbor perspectives in medicine.,* **2015**, *5*(9), 17-30.
13. Migliori G.B.; Sotgiu G.; Arcy Richardson M.; Centis R.; Facchini A.; Guenther., *European Respiratory Journal*., **2009**, *34*(3), 778-790.
14. Gaba M.; Punam G.; Sarbjot S., *International Journal of Drug Development and Research.,* **2010**, *2*, 219-231.
15. Meng X.Y.; Zhang H.X.; Mezei M.; *Cui M., Curr Comput Aided Drug Des*., **2011**, *7*(2), 146-157.